SI Appendix

Catalytic amino acid production from biomass-derived intermediates

Weiping Deng[a,b,1], Yunzhu Wang[a,1], Sui Zhang[a], Krishna M. Gupta[a], Max J. Hülsey[a], Hiroyuki Asakura[c,d], Lingmei Liu[e], Yu Han[e], Eric M. Karp[f], Gregg T. Beckham[f], Paul J. Dyson[g], Jianwen Jiang[a], Tsunehiro Tanaka[c,d], Ye Wang[b], and Ning Yan[a,2]

[a]Department of Chemical and Biomolecular Engineering, National University of Singapore, 4 Engineering Drive 4, Singapore 117585 Singapore; [b]State of State Key Laboratory for Physical Chemistry of Solid Surfaces, College of Chemistry and Chemical Engineering, Xiamen University, Xiamen 361005 China; [c]Department of Molecular Engineering, Graduate School of Engineering, Kyoto University, Kyoto 615-8510 Japan; [d]Elements Strategy Initiative for Catalysts & Batteries (ESICB), Kyoto University, Kyoto 615-8245 Japan; [e]King Abdullah University of Science and Technology (KAUST), Advanced Membranes and Porous Materials Center, Physical Sciences and Engineering Division, Thuwal, 23955-6900 Saudi Arabia; [f]National Bioenergy Center, National Renewable Energy Laboratory, 15013 Denver W Pkwy, Golden, CO 80401, USA; and [g]Institut des Sciences et Ingénierie Chimiques, École Polytechnique Fédérale de Lausanne (EPFL), CH 1015 Lausanne, Switzerland

[1]W.D. and Yunzhu Wang contributed equally to this work.
[2]To whom correspondence may be addressed. Email: ning.yan@nus.edu.sg

1

Supplementary Experimental Procedures

I. Materials

Carbon nanotubes (ø: 20-40 nm; 70~120 m^2/g) were purchased from Shenzhen Nanotech Port Co., Ltd. Ruthenium chloride ($RuCl_3 \cdot xH_2O$, ~37% Ru basis), palladium chloride ($PdCl_2$, $\geq$ 59.5% Pd basis), chloroplatinic acid hydrate($H_2PtCl_6 \cdot xH_2O$, ~38% Pt basis), Rhodium chloride hydrate ($RhCl_3 \cdot xH_2O$, 38.5%~45% Rh basis), silica (SiO_2 fumed, 0.2~0.3 μm), Al_2O_3 (activated, neutral), CeO_2 (powder), Ru/C (Ru, 5 wt %), DL-lactic acid (~90%), 3-Phenyllactic acid (99%), α-hydroxyl butyric acid (98%), 3-methylbutyric acid (99%), α-hydroxyisoproic acid (99%), α-hydroxysuccinic acid (99%), pyruvic acid (98%), α-hydroxyl isobutyric acid (99%), L-alanine (98%), 3-hydroxybutyric acid (95%), 3-hydroxypropionic acid (30% solution in water) and aquous ammonia solution (25 wt % NH_3) were provided by Sigma Aldrich. Iridium chloride hydrate ($IrCl_3 \cdot xH_2O$, 60% Ir basis) was obtained from Shaanxi Kaida Chemical Engineering Co., Ltd. All the chemcials were used as received.

II. Catalysts characterization

TEM was performed on a JEM 2100F (JEOL, Japan) microscope operated at 200 kV. Samples for TEM measurements were suspended in ethanol and dispersed ultrasonically. Drops of suspensions were applied on a copper grid coated with carbon. STEM images were obtained on a Cs-corrected FEI Titan G2 60–300 Microscope operated at 300 kV using a HAADF detector. Probe Cs corrector was applied to get better spatial resolution. XRD analysis was carried out using a Bruker D8 Advance X-Ray Diffractometer, at a scan rate of 2 °/min. It was operated at 40 kV applying a potential current of 30 mA. XPS were recorded on a VG Escalab MKII spectrometer, using a mono Al Kα X-ray source (hν = 1486.71 eV, 5 mA, 15 kV), and the calibration was done by setting the C1s peak at 284.6 eV.

Ru K-edge XAS of the Ru catalysts and Ru powder as well as RuO_2 were recorded at the BL01B1 beamline at SPring-8 (Japan Synchrotron Radiation Research Institute, Hyogo, Japan) in the transmission mode at ambient temperature. A Si(3 1 1)double crystal monochromator was used to obtain a monochromatic X-ray beam. The photon energy was calibrated at the inflection point of the Ru K-edge XANES spectrum of Ru metal powder to 22118 eV. Higher harmonics X-rays were removed by setting the glancing angle of Rh-coated X-ray mirrors to 1.5 mrad. Incident (I_0) and transmitted (I_1) X-ray fluxes were measured with ion chambers filled with N_2(50%)/Ar(50%) and Ar(75%)/Kr(25%), respectively. Data reduction and analysis were done using Athena and Artemis as included in the Ifeffit and Demeter program package. Theoretical scattering paths were created with FEFF6.0L for curve-fitting analysis and amplitude reduction factors were estimated from reference samples. After Fourier transformation of the k^3-weigthed EXAFS oscillation in the range of 3.0–15.0 Å, curve-fitting analyses were done from 1.0–2.7 $Å^{-1}$ in R space.

H_2 chemisorption experiment was conducted on a ChemBET Pulsar TPR/TPD (Quantachrome). 100 mg freshly reduced Ru/CNT catalyst was heated at 923 K under N_2 for 0.5 h to remove the hydrogen adsorbed on Ru atoms. After that, the temperature was reduced to 423 K, and waited until baseline became stable. Subsequently, successive doses of H_2 gas were provided through a calibrated injection valve (159 μL H_2 $pulse^{-1}$) at 423 K. The injection would end when the intensities of three peaks in a row keep constant. We assume the chemisorption follows this equation: Ru (surface) + 1/2 H_2 = RuH (surface). Thus, the dispersion of Ru (d_{Ru}) is calculated using the formula: $d_{Ru} = 2*n(H_2)/n_{total}(Ru)$.

Metal leaching in the solution after hot filtration was determined by iCAP 6000 Series inductively coupled plasma atomic emission spectroscopy (ICP-OES) and Agilent Technologies 7500 series ICP-MS.

III. General experimental procedure

For recycling experiment, the catalyst was washed with deionized water after reaction and centrifuged for three times. The washed catalyst was dried in an oven at 343 K overnight for the next usage.

Hot filtration was conducted to examine the catalytic activity of reaction solution. After 1 hr of reaction (0.5 mmol lactic acid, 50 mg 3 wt % Ru/CNT, 2.5 mL 25 wt % NH_3H_2O, 1 MPa H_2, 493 K), gas was released after cooling the reactor to room temperature. The reaction mixture was then heated to 353 K (before water boils), and immediately filtrated by a filter (0.45 µm). The reactor was washed with pre-heated deionized water (353 K) for two times, and immediately filtered. The collected liquid was cooled to room temperature, and aqueous ammonia (25 wt %) was added to make the total volume back to 2.5 mL. The solution was then transferred to a clean reactor, and further reacted for either 0.5 h or 1 h, at 493 K in the presence of 1 MPa H_2.

To evaluate the leaching level of Ru, a third hot filtration experiment was conducted after 2 h reaction (following the same protocol as above). ca. 0.5 mL solution after hot filtration (out of ca. 2.5 mL) was digested in concentrated nitric acid (68% HNO_3) at 393 K for 2 h and then diluted with deionized water to 25 mL. The solution was first tested with ICP-OES and the Ru concentration was below the detection limit. It was further sent for ICP-MS analysis where a small amount of Ru in the solution was identified (0.042 ppm). This number translates to 5.5 µg leached Ru in the solution, corresponding to 0.37 wt % of total Ru in the Ru/CNT catalyst.

Amino acids were analyzed on HPLC with a C8 column by using a precolumn derivatization method, where ortho-phthalaldehyde was used as the derivatization reagent. However, the peak for derivatized phenylalanine was overlapped with derivatized ammonia in the solution, and therefore ammonia should be removed prior to the derivatization for this compound. After conversion of 3-phenyllactic acid, the solution was treated in a rotary evaporator. Most of ammonia was removed after 1.5 h at 140 mbar and 318 K. The solution was then freeze-dried to remove the remaining ammonia before derivatization.

Supplementary Data Items

I. Characterizations

(1) XRD patterns and TEM images of different metal catalysts loaded on CNT

As shown in Fig. S1, CNT has two characteristic reflection peaks at 26.1° and 42.6°, corresponding to the (200) and (100) facets, respectively. After loading different metals, the reflection peaks attributed to CNT sustained for all supported catalysts. No sharp peak of the noble metals (generally at 2theta = ~40°) could be observed for these catalysts, suggesting that all the noble metals were well dispersed on CNT support, which was supported by TEM micrographs in Fig. S2. These observations could help to exclude the dispersion and size effects on the catalytic performance of different catalysts.
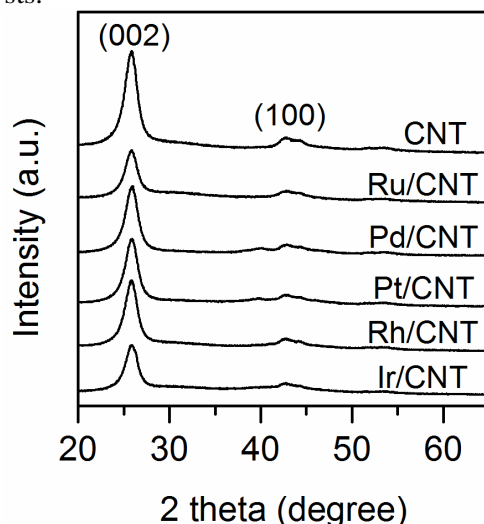
**Fig. S1.** XRD patterns of different metal catalysts loaded on CNT
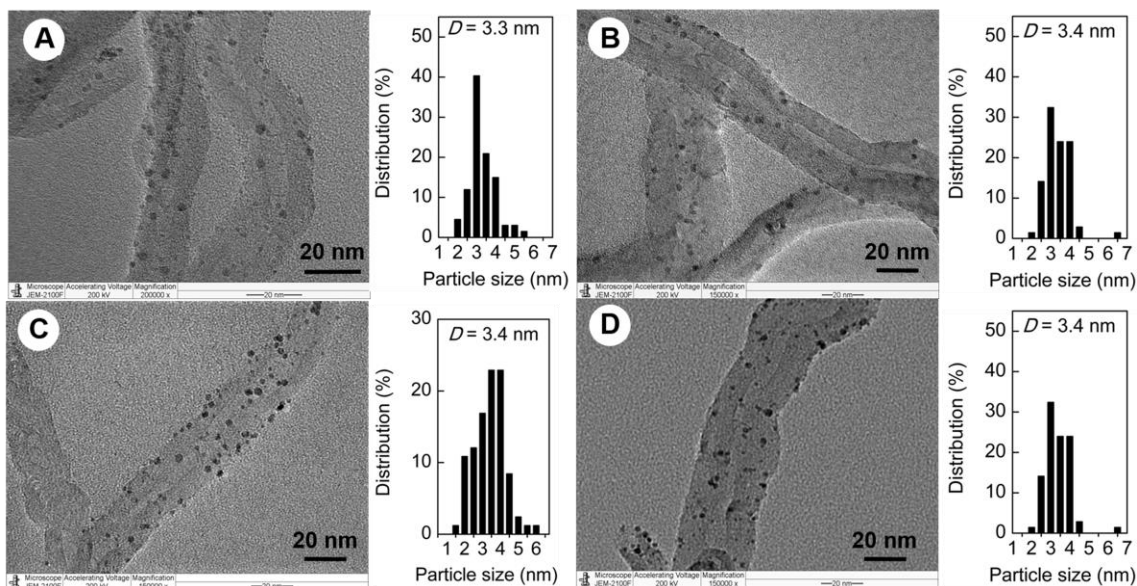
Fig. S2. TEM micrographs of different metal catalysts loaded on CNT. (*A*) Ru/CNT, (*B*) Pd/CNT, (*C*) Pt/CNT and (*D*) Ir/CNT.

(2) H$_2$ chemisorption of Ru/CNT catalyst
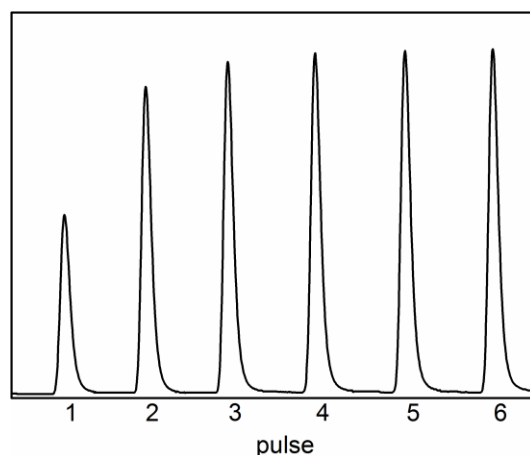
Fig. S3. H$_2$ chemisorption profile of Ru/CNT catalyst. Catalyst loading: 100 mg. 159 μL H$_2$ per pulse. 423 K. The dispersion of Ru on Ru/CNT is 24.3% based on chemisorption data.

(3) TEM micrographs of Ru(OH)$_x$/CNT catalysts

Fig. S4 shows that Ru species are amorphously dispersed on CNT in the Ru(OH)$_x$/CNT catalyst. After reaction, Ru nanoparticles have been formed, corroborating the transformation of Ru morphology.
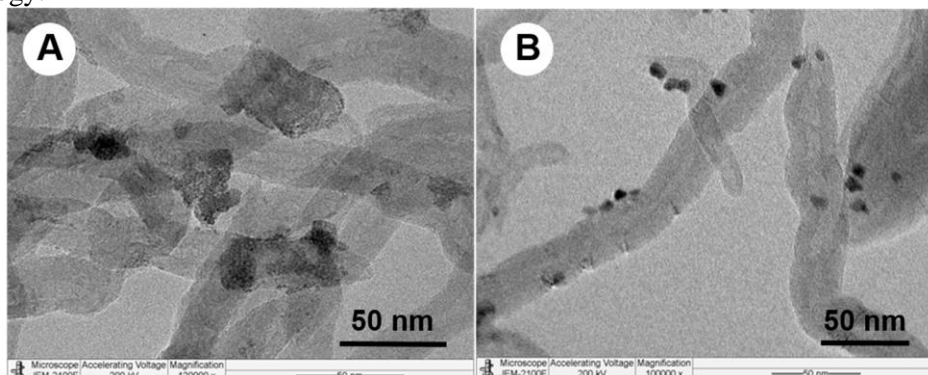

Fig. S4. TEM micrographs. (*A*) Ru(OH)$_x$/CNT and (*B*) the spent Ru(OH)$_x$/CNT.

II. Control experiments

(1) Ru/CNT catalyzed conversion of α-hydroxyl isobutyric acid

Table S1. Catalytic performance of Ru/CNT for amination of α-hydroxyl isobutyric acid

Temperature (K)	Conversion (%)	α-Amino isobutyric acid yield (%)
473	60	-
493	66	-
513	74	-

Reaction conditions: 0.5 mmol α-hydroxyl isobutyric acid, 50 mg Ru/CNT (Ru loading 3 wt %), 2.5 mL NH$_3$H$_2$O (25 wt %), 1 MPa H$_2$, 2 h.

(2) The effect of H$_2$ pressure on the amination of lactic acid

Table S2. The effect of hydrogen pressure on the catalytic performance of Ru/CNT for lactic acid amination

H$_2$ pressure (MPa)	Conversion (%)	Alanine yield (%)
0	51	27
0.05	67	41
0.2	70	47
1	75	49

Reaction conditions: 0.5 mmol lactic acid, 50 mg Ru/CNT (Ru loading 3 wt %), 2.5 mL NH$_3$H$_2$O (25 wt %), 493 K, 2 h.

(3) The conversion of pyruvic acid and alanine

Table S3. Catalytic conversion of pyruvic acid and alanine over different metal catalysts

Substrate	Catalyst	Temperature (K)	Conversion (%)	Alanine yield (%)	Lactic acid yield (%)
Pyruvic acid	none	373	100	3.7	0
	Ru/CNT		100	61	3.4
	Pd/CNT		100	52	1
	Pt/CNT		100	52	12
	Ir/CNT		100	66	3
	Rh/CNT		100	64	2
Alanine	none	493	17	-	0
	Ru/CNT		36	-	10
	Pd/CNT		20	-	0

Reaction conditions: 0.5 mmol substrate, 50 mg catalyst (metal loading 3 wt %), 2.5 mL NH$_3$H$_2$O (25 wt %), 1 MPa H$_2$, 2 h.

(4) The dehydrogenation properties of commercial Ru/C and Pt/CNT catalysts

To check whether other Ru catalysts have the similar behavior as Ru/CNT, we investigated the commercial Ru/C (5 wt %) catalyst for the conversion of isopropanol. Pt/CNT, another platinum-group metal catalyst was also studied for comparison. Fig. S5 displays that the NH_3 has a significant enhancement effect on the dehydrogenation of isopropanol over a commercial Ru/C catalyst, but a negative effect on the catalytic performance of Pt/CNT. This further confirmed the superior property of Ru species for dehydrogenation in the presence of NH_3.
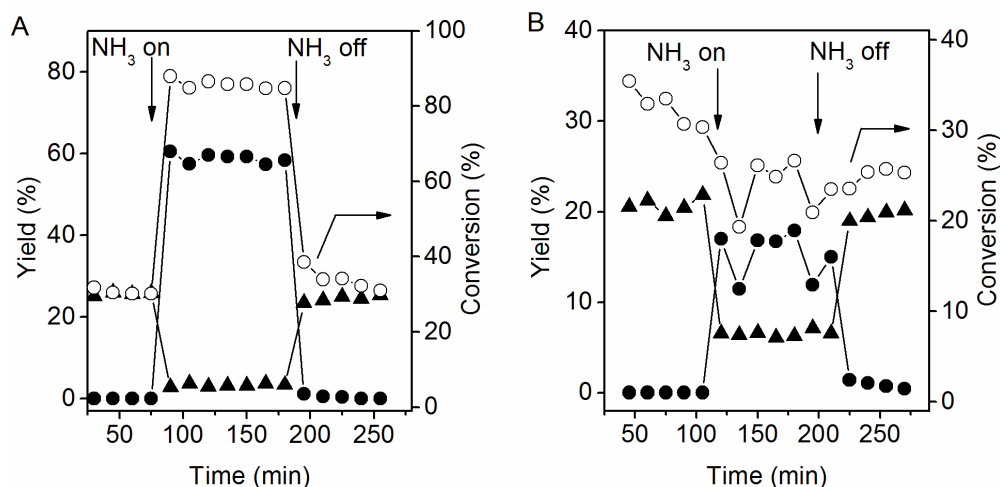

Fig. S5. Dehydrogenation of isopropanol over (*A*) commercial Ru/C and (*B*) Pt/CNT under H_2 atmosphere. (○) isopropanol conversion, (▲) acetone yield, (●) isopropylamine yield. Reaction conditions: 50 mg catalyst (metal loading 3 wt %), 2 μL/min isopropanol, 50 mL/min total flow rate, 473 K, 8 mL/min NH_3 flow.

(5) The effect of ethylenediamine on Ru/CNT, Pd/CNT and Pt/CNT over hydrogenation of acetophenone.

Table S4. Catalytic hydrogenation of acetophenone over different metal catalysts

Entry	Catalyst	Conversion (%)	Yield (%)			
			A	**B**	**C**	**D**
1	Ru/CNT	27	21	1	4	1
2*		69	69	0	0	0
3	Pd/CNT	70	61	0	9	0
4*		27	27	0	0	0
5	Pt/CNT	63	59	0	2	2
6*		74	74	0	0	0

Reaction conditions: 5 mmol acetophenone, metal/acetophenone molar ratio = 0.002, 3 mL isopropanol, 0.4 MPa H_2, 333 K, 2 h. (**A**) 1-Phenylethanol, (**B**) ethylcyclohexane, (**C**) ethylbenzene, (**D**) 1-cyclohexylethanone.
*Ethylenediamine (1 mmol) and KOH (2 mmol) were added into the reaction solution.

7

(6) Reaction condition optimization and catalytic activity of hot filtrate

After 1 h reaction, hot filtration was conducted at 353 K. The hot filtrate then was added to the reactor that had been pre-charged with aqueous ammonia. The reactor was charged with 1 MPa H_2 and heated at 493 K for 0.5 h and 1 h respectively. The yield of alanine decreased with prolonged reaction time, indicating the hot filtrate did not have catalytic activity.
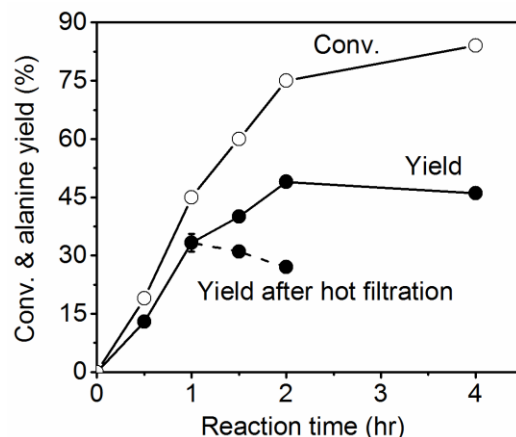

Fig. S6. Time course for the catalytic conversion of lactic acid. Error bar of yield at 1 h indicate SDs. Reaction conditions: 0.5 mmol lactic acid, 50 mg Ru/CNT (Ru loading 3 wt %), 2.5 mL NH_3H_2O (25 wt %), 1 MPa H_2, 493 K.
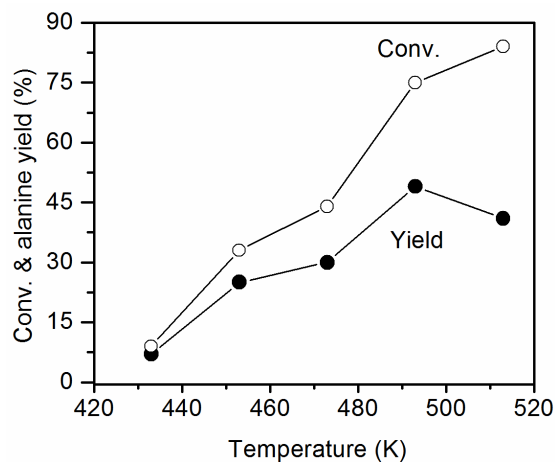

Fig. S7. Temperature effect on Ru/CNT catalyzed conversion of lactic acid. Reaction conditions: 0.5 mmol lactic acid, 50 mg Ru/CNT (Ru loading 3 wt %), 2.5 mL NH_3H_2O (25 wt %), 1 MPa H_2, 2 h.

8

(7) Recycling experiments (Ru/CNT)

Table S5. Recycling Ru/CNT catalyst in conversion of lactic acid to alanine

Catalytic cycle	Catalyst amount (mg)	Accumulated turnover number[*]
1	50.0	68
2	48.9	137
3	48.0	206
4	47.3	276
5	46.2	336
6	46.0	397
7	44.7	457
8	43.2	515
9	41.6	575

Reaction conditions: 0.5 mmol lactic acid, Ru/CNT (Ru loading 3 wt %), 2.5 mL NH_3H_2O (25 wt %), 1 MPa H_2, 493 K, 2 h.
[*]Turnover number of each catalytic cycle was calculated based on initial Ru dispersion measured by H_2 chemisorption (24.3%).

(8) Recycling experiments (Ru(OH)$_x$/CNT)
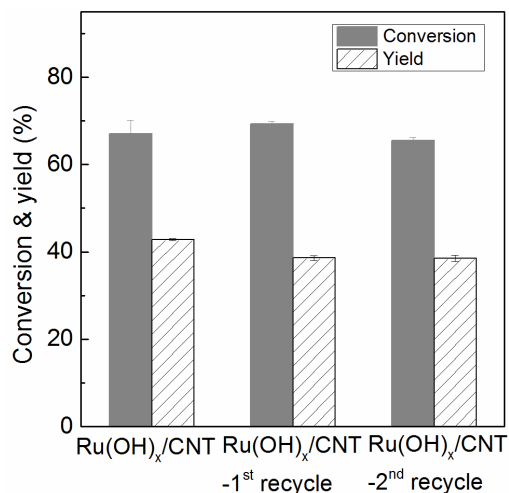
Fig. S8. Recycling Ru(OH)$_x$/CNT catalyst in conversion of lactic acid to alanine. Reaction conditions: 0.5 mmol lactic acid, 50 mg Ru(OH)$_x$/CNT (Ru loading 3 wt %), 2.5 mL NH_3H_2O (25 wt %), 1 MPa H_2, 493 K, 2 h. Error bars indicate SDs.

(9) Modification of Ru/CNT with second metal

Table S6. Catalytic performances of modified Ru/CNT for conversion of lactic acid

Entry	CNT supported catalyst	Conversion (%)	Alanine yield (%)
1	Ru-Ni	88	57
2	Ru-Co	39	25
3	Ru-Pd	63	35
4	Ru-Au	82	37
5	Ru-Pt	57	29
6	Ru-Cu	31	17
7	Ru-Zn	85	49
8	Ru-Fe	52	34
9	Ru-Sn	70	42

Reaction conditions: 0.5 mmol lactic acid, Ru/lactic acid molar ratio = 0.025, 2.5 mL NH_3H_2O (25 wt %), 1 MPa H_2, 493 K, 2 h. Ru/second metal molar ratio = 1/1.

Table S7. Catalytic performances of Ni modified Ru/CNT for conversion of lactic acid

Entry	Temperature and time	Conversion [%]	Alanine yield [%]
1	453 K, 2 h	41	29
2	473 K, 2 h	80	62
3	473 K, 4 h	88	60
4	493 K, 2 h	88	57
5	513 K, 2 h	87	36

Reaction conditions: 0.5 mmol lactic acid, Ru/lactic acid molar ratio = 0.025, 2.5 mL NH_3H_2O (25 wt %), 1 MPa H_2. Ru/Ni molar ratio = 1/1.

Table S8. Catalytic performances of Ni modified Ru/CNT for conversion of lactic acid

Entry	Ni loading [wt %]	Conversion [%]	Alanine yield [%]
1	1	83	54
2	2	87	56
3	5	85	59
4	10	88	62

Reaction conditions: 0.5 mmol lactic acid, 50 mg Ru/CNT (Ru loading 3 wt %), 2.5 mL NH_3H_2O (25 wt %), 1 MPa H_2, 493 K, 2 h.

III. Two-step synthesis of alanine from glucose

Table S9. Catalytic conversion of glucose to lactic acid and lactic acid to alanine

Step	Conversion* (%)	Yield* (%)				
		Alanine	Lactic acid	Fructose	Glyceraldehyde	Glyceric acid
1[†]	100	-	75	1	6	6
2[‡]	-	43	19	0	0	2

*The conversion and yields are calculated based on glucose.
[†]Reaction conditions: 0.25 mmol glucose, 2.5 mmol Ba(OH)$_2$, 10 mL H$_2$O, 0.1 MPa N$_2$, 298 K, 48 h.
[‡]Reaction conditions: 100 mg Ru/CNT (Ru loading 3 wt %) modified by 10 wt % Ni, 2.5 mL NH$_3$H$_2$O (25 wt %), 1 MPa H$_2$, 493 K, 2 h.

IV. Promotional effect of Ni and alkaline on catalytic conversion of hydroxyl acids

Table S10. Promotional effect of Ni or alkaline on catalytic conversion of α-hydroxyl acids

Substrate	Product		Condition	Yield (%)
		Alanine	1 mmol KOH	60
		α-Aminobutyric acid	1 mmol KOH	63
		Valine	1 mmol KOH	60
		Leucine	10 wt % Ni	58
		Aspartic acid	-	11
			10 wt % Ni	18
		Phenylalanine*	-	5
			1 mmol KOH	10
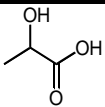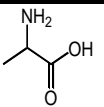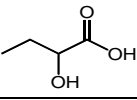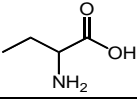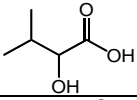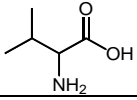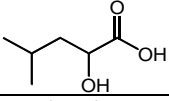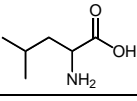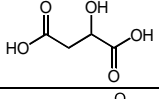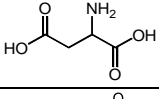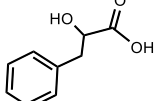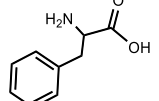
Reaction conditions: 0.5 mmol lactic acid, 50 mg Ru/CNT (Ru loading 3 wt %), 2.5 mL NH$_3$H$_2$O (25 wt %), 1 MPa H$_2$, 493 K, 2 h.
*Ammonia was removed prior to derivatization.

V. Catalytic conversion of β-hydroxyl acids to β-amino acids

Table S11. Catalytic conversion of β-hydroxyl acids to β-amino acids

Substrate	Product		Yield (%)
HO–CH$_2$CH$_2$–C(O)OH	H$_2$N–CH$_2$CH$_2$–C(O)OH	β-Alanine	2.3
CH$_3$CH(OH)CH$_2$–C(O)OH	CH$_3$CH(NH$_2$)CH$_2$–C(O)OH	β-Aminobutyric acid	3.3
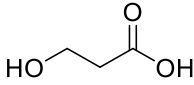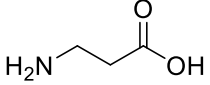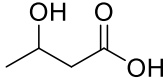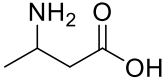
Reaction conditions: 0.5 mmol substrate, 50 mg Ru/CNT (Ru loading 3 wt %), Ru/CNT was modified with 10 wt % Ni, 2.5 mL NH$_3$H$_2$O (25 wt %), 1 MPa H$_2$, 493 K, 2 h.

VI. Membrane distillation for the purification of alanine

(1) Methods

A membrane distillation unit was employed to separate alanine from ammonia and water. As illustrated in Fig. S9, the feed solution containing 2 wt/vol % alanine in 25 wt % ammonia water was heated to the desired temperature and circulated along the shell side of the membrane. Cold water stream was circulated at the lumen side, the temperature of which was kept at 12 °C by a cooler. Due to the difference in partial vapor pressure, vaporized ammonia and water pass through the pores of the membrane and were condensed in the cold stream. A hydrophobic tribore polyvinylidene fluoride hollow fiber membrane was prepared by a method similar to reference (1) and used as the separation barrier, with an effective membrane area of 8.2 cm^2. The initial volume of the feed and cold water was each 100 mL. The feed solution was heated firstly to 40 °C for 2 hours to allow a large portion of ammonia to pass through and then kept at 46 °C until the desired recovery was reached. The final feed volume was recorded and the final alanine concentration in the feed was measured by a HPLC method.
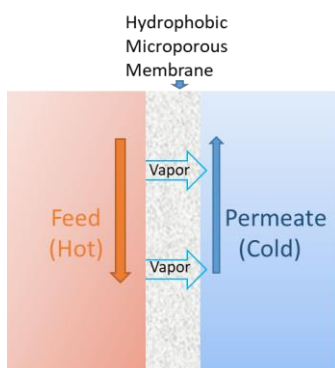

Fig. S9. An illustration of the membrane distillation unit, where the hydrophobic microporous membrane is placed in the middle, the hot feed solution is flowing through one side of the membrane, and vapor passes through the pores of the membrane and condenses in the cold permeate stream at the other side.

The retention (R, %) of alanine was calculated based on eq. (S1):

$$R = \frac{c_{a,f}}{c_{a,i}} \times 100\% \tag{S1}$$

where $C_{a,f}$ and $C_{a,i}$ are the final and initial concentrations of alanine in the feed, respectively.

The recovery (Rc, %) of the feed solution was obtained from eq. (S2):

$$Rc = (1 - \frac{V_{a,f}}{V_{a,i}}) \times 100\% \qquad (S2)$$

where $V_{a,f}$ and $V_{a,i}$ are the final and initial volumes of the feed, respectively.

The average permeation flux (J) is related to the permeated volume, membrane area (A_m) and duration (Δt) by eq. (S3):

$$J = \frac{V_{a,f} - V_{a,i}}{A_m \Delta t} \qquad (S3)$$

(2)   Results and energy comparison

The membrane distillation process was ceased at the recovery rate of 74%, as a minimum volume is required to keep the flow continuous. Higher recovery can be achieved if a larger initial volume is supplied. Alanine was retained within the feed solution by almost 100%, and its concentration was increased from 0.02 g/mL to 0.077 g/mL. The average permeation flux was 10 L m^{-2} h^{-1}.

Traditional distillation processes require the removal of noncondensable gases by vacuum, which consumes significant amount of energy (2). To improve the efficiency, evaporators based on the convection or circulation of water-saturated air have been designed. Their efficiency is inversely related to the gap between evaporation and condensation surfaces, and yet it is difficult to reduce the gap without contaminating the permeate by the feed (2). In the membrane distillation process, hydrophobic microporous membranes provide a very thin interface of tens to hundreds of micrometers between the two surfaces, which also create a large contact area within the microporous structure to promote an efficient mass transfer. As a result, it is possible to operate the system at a lower temperature.

Apart from direct energy saving of membrane distillation compared with direct distillation (5-10%), the major benefit of the former is the lower operating temperature that enables the use of low-grade waste heat. The US Department of Energy has estimated that 20–50% of the energy consumed during industrial manufacturing processes is lost as waste heat, with 60% as the low-grade waste heat (whose temperature falls below 230 °C by definition) (3). In our system, for instance, the catalytic production of amino acids is conducted at 220 °C, which can easily serve as the heating source for the MD separation process. Through the use of the waste heat from the reaction system, no additional energy is required for heating in MD and hence saves 50% of the total energy. Overall, the MD process can potentially saves energy by two to three times.

Supplementary References

1. Lu KJ, Zuo J, Chung TS (2016) Tri-bore PVDF hollow fibers with a super- hydrophobic coating for membrane distillation. *J Membr Sci* 514: 165–175.
2. Drioli E, Molero LP, Criscuoli A (2000) Membrane Distillation. *EOLSS Encycl. Water and wastewater treatment technologies* volume III.
3. Waste heat recovery: technology and opportunities in U.S. industry (2008). Department of Energy. Industrial technologies program.